Pulsed CMT Process Improves Mechanical Properties of Al 6061-T6 and SS 304 Lap Joints for Automotive

Md Anwar(✉) and R. Rajendra

Department of Mechanical Engineering, University College of Engineering, Osmania University, Hyderabad, India
anw246@gmail.com

Abstract. Automotive manufacturers are facing greater demands to improve the fuel efficiency and performance of their vehicles while also reducing the overall weight. In order to meet these challenges, manufacturers are turning to alternative materials such as stainless steel and aluminium for their vehicle structures. This research study focused on welding and brazing Al 6061-T6 and SS 304 with different thicknesses and lap joints using the pulse Cold Metal Transfer (PCMT) process. The goal was to evaluate the mechanical properties of the joints, specifically the tensile-shear strength and microhardness, and to characterize the macro and microstructures using Optical microscopy and SEM. The results show that by varied welding parameters and found that the bead width (BW) and contact angle (CA) depend on heat input (HI) and the combination of parameters used. Increasing HI generally led to higher bead width and lower contact angle. Increasing welding travel (WT) and decreasing interval time resulted in higher microhardness values of the heat affected zone (HAZ) and fusion zone (FZ). The microhardness of the HAZ of both materials varied with input parameters, with increasing welding travel and decreasing interval time resulting in higher maximum loads, maximum stresses, and yield stresses. The tensile strength of the joint was influenced by the microstructure and microhardness values of the welded joint, with the highest values obtained in Trial T8. The fusion zones had corrugated and curved shapes and were more prominent at the joints, while the Intermetallic compound (IMC) at the Al 6061-T6 and SS 304 interact were less than 10 microns.

Keywords: Pulsed Cold Metal Transfer (PCMT) · Heat Input (HI) · Contact Angle (CA) · Heat Affected Zone (HAZ) · Fusion Zone (FZ) · Intermetallic Compound (IMC) · Dissimilar Metal and Welding Travel (WT)

1 Introduction

The use of lightweight materials in the automobile industry has become increasingly popular due to the need to reduce pollution and save energy [1]. Among these materials, aluminium alloys are widely used due to their low density and high specific strength capacity [2]. One of the challenges associated with the use of aluminium in vehicle

B. Raj et al. (Eds.): ICETE 2023, AER 223, pp. 1159–1171, 2023.
https://doi.org/10.2991/978-94-6463-252-1_116

bodies is joining it to steel, which offers the potential for selectively replacing steel parts with lighter aluminium parts, leading to further weight reduction in vehicle bodies [3]. Several techniques have been reported in the literature for joining aluminium alloys to steel, including arc welding with MIG, TIG welding, MIG/TIG double-sided welding, cold metal transfer (CMT) welding, ultrasonic welding, laser brazing, and friction stir welding [4–12]. However, the bond strength can be negatively affected during fusion bonding due to the formation of brittle intermetallic compounds (IMCs) at the interact between aluminium and steel [13]. Recent studies indicate that IMC layers below 10 μm do not significantly affect bond strength [14]. Therefore, the use of energy-efficient fusion techniques such as laser brazing or CMT welding is recommended to control the thickness of the IMC layer at the Al-steel interact [15, 16]. CMT welding, which integrates welding wire movement with process control and operates in short circuit mode, is advantageous due to its spatter-free welding, stable arcs, and low energy input, making it suitable for joining thin sheets and dissimilar materials [17, 18]. The strength of the joint between aluminium alloy Al 6061-T6 and galvanized steel with 4043 filler during CMT spot welding is dependent on the weld area, and joint strength of up to 304 MPa has been reported with AlSi3Mn1 filler wire [19].

In this study, PCMT welding was used to lap weld dissimilar materials, namely 6061-T6 aluminium alloy and 304 stainless steel, with a focus on controlling the weld metal droplet per second and interval time to minimize HI. The macromorphology, micro hardness, microstructure, and interact layer thickness of the PCMT welding joints were analyzed to determine the relationship and effective control mechanism among welding parameters, HI, and interact layer thickness. These findings are valuable for enhancing the joint strength of aluminium and stainless steel materials.

2 Experimental Setup and Procedure

2.1 Selecting Process Parameters

The study aimed to investigate the weldability of aluminum alloy (Al 6061-T6) and electrolyte zinc coating stainless steel 304 (SS 304) using the CMT pulse lap welding technique. The dimensions of the base materials were 200 × 100 × 2 mm for aluminum and 200 × 100 × 1.5 mm for stainless steel, with an overlap width of 10 mm. The FM used was ER4043 flux cored wire with a diameter of 1.2 mm.

The electrolyte Zn coating selected to improve the wettability of the molten FM in pulse CMT welding was a Zn coating with a thickness of 6.8 μm for SS 304. The welding equipment used was the Fronius-500i pulsed CMT welding machine, and the shielding gas used was argon with a purity of 99.99%. The welding parameters included a gas flow rate of 15 L per min, a distance between the contact tip to work distance of 15 mm, a torch angle of 60 degrees, and a traverse angle of 150 degrees. To regulate the welding speed, interval time, and CMT cycle in a unified adjustment mode based on the base and filler materials, a welding database was selected. Tables 1 and 2 provided the chemical compositions and mechanical properties of the base materials, AA6061-T6, SS304, and ER4043, respectively. Figure 1 depicted the welding experiment system setup, which involved the use of the Fronius-500i pulsed CMT welding machine as the power source, along with the kuku robot. After welding, macro and microstructures were observed

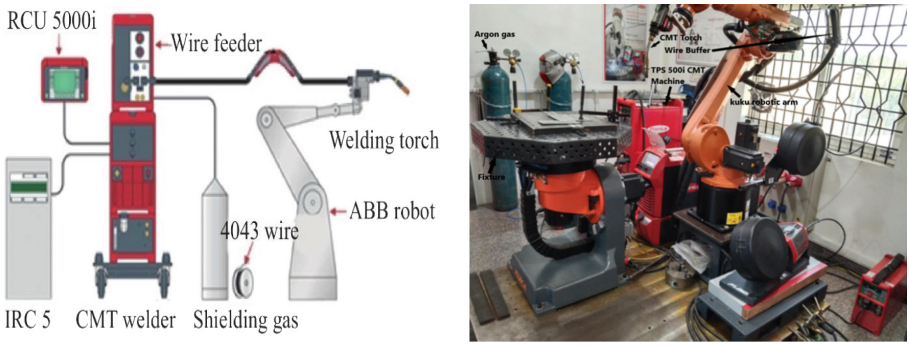

Fig. 1. The pulsed CMT welding experimental setup (Fronius India Pvt. Ltd., Bengaluru).

Table 1. Chemical composition of materials (wt.%)

Material	C	Si	Mn	S	P	Mg	Zn	Cu	Cr	Ni	Ti	Fe	Al
AA6061-T6	-	0.45	0.11	-	-	0.9	0.10	0.17	0.14	-	0.15	0.4	Bal.
SS 304	0.08	0.75	2.0	0.03	0.045	-	-	-	16.5	13.0	-	Bal.	-
ER 4043	-	5.6	0.05	-	-	0.05	0.1	0.3	-	-	0.2	0.8	Bal.

with optical microscopes, and the thickness of the interfacial layers was measured with Digimizer software. Tensile-shear strength was tested at room temperature using Instron 6800 universal tensile equipment, and the tests were carried out according to the ASME Section 9 standard of the universal testing machine. The transverse tensile specimens had a size of 100 × 10 mm, and the stroke speed was set to 1 mm/min. The microhardness distribution was measured using the Qualitest FM-310 and represented the mechanical properties of the joint, as well as reflected the structural evolution of the fusion zone, HAZ, and base material.

The chemical composition of the base materials and FM provided insights into their properties and the possible outcomes of their combination. AA6061-T6 had a magnesium content of 0.9%, which made it susceptible to galvanic corrosion when combined with SS 304, as the latter contained a significant amount of chromium and nickel. SS 304 had a low carbon content, which made it resistant to sensitization, and a high nickel content, which contributed to its corrosion resistance. ER4043 FM had a high silicon content, which improved the fluidity of the molten metal and reduced porosity.

3 Results and Discussion

3.1 Microstructure of Fusion Zone of Al 6061-T6 and SS 304

The microstructure of the fusion zone of Al 6061-T6 and SS 304 was studied by adjusting the welding speed, interval time, and CMT cycle. The study aimed to optimize the welding process and investigate the influence of process parameters on various aspects

Table 2. Mechanical properties of the base materials.

Material	Yield strength MPa	Tensile strength MPa	Elongation A%
AA6061-T6	241	262	14
SS304	218	525	24

Table 3: Pulsed CMT process parameters L9 orthogonal array as per DoE (Minitab).

Trials No.	T1	T2	T3	T4	T5	T6	T7	T8	T9
Welding Speed (m/min)	0.40	0.40	0.40	0.45	0.45	0.45	0.50	0.50	0.50
Interval time (sec)	0.08	0.10	0.12	0.10	0.12	0.08	0.12	0.08	0.10
CMT Cycle	4	5	6	6	4	5	5	6	4

of the joints. Table 3 outlines the adjustable parameters and their respective values. Figure 2 illustrates the macrographs of the welds and cross-sections. The study also revealed that the wettability of the molten aluminum alloy on the stainless steel surface improved with increasing HI during welding, which resulted in a wider scattering width. The study also examined the microstructure, hardness, and tensile strength of the joints.

These levels and factors are significant for the pulsed CMT process for L9 OA as they can affect the welding outcome. By adjusting the levels for each parameter, the process can be optimized to produce the desired results. For instance, the welding travel speed can affect the amount of heat input and the speed of the welding process, while the interval time can affect the cooling time and the formation of the weld pool. Lastly, the CMT cycle can impact the deposition rate and the heat input.

Table 4 shows the effect of HI on bead width and contact angle of Al 6061-SS304 joints produced using different combinations of welding parameters. The welding speed, interval time, and CMT cycle were varied to produce a total of nine different joints. The HI (Q) for each joint was also recorded and used to evaluate the effect of HI on the bead width and contact angle.

The results show that the bead width and contact angle are dependent on the HI and the combination of welding parameters used. For example, joint T8 produced with a welding travel of 0.50 m/min, interval duration of 0.08 s, and CMT cycle stage of 6 had the largest bead width of 8.43 mm and the smallest contact angle of 38 degrees. On the other hand, joint T5 produced with a welding travel of 0.45 m/min, interval duration of 0.12 s, and CMT cycle stage of 4 had the smallest bead width of 6.72 mm and the largest contact angle of 74 degrees.

The results suggest that increasing the HI generally leads to an increase in the bead width, which is expected since more HI results in more melting and spreading of the molten metal. Figure 3 shown that the macroscopic images of a lap joint pulse CMT

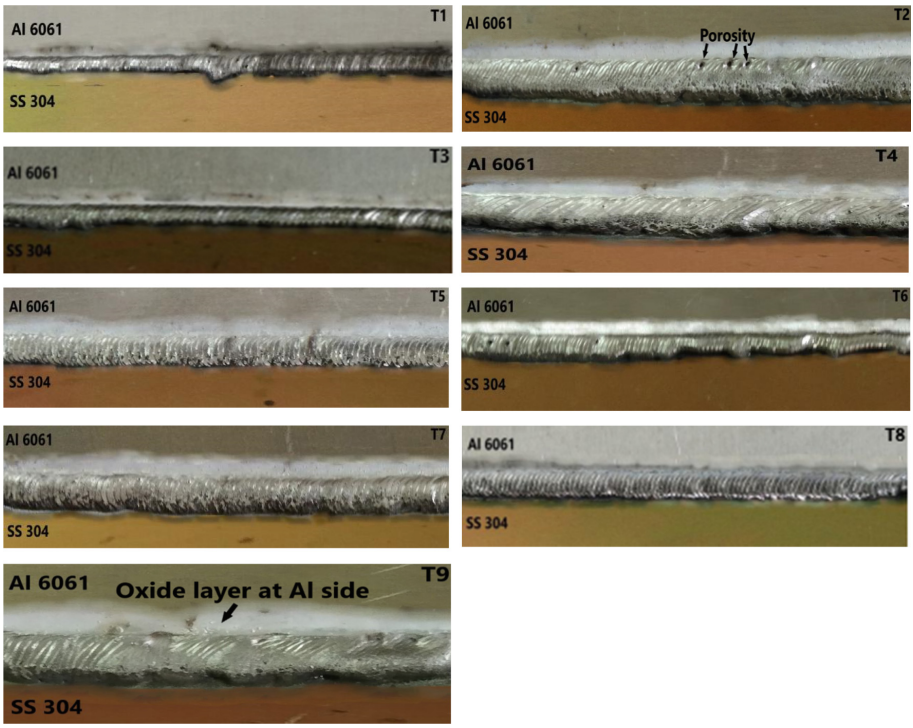

Fig. 2: Cross-sectional morphology of fusion zones with varying CMT welding parameters.

Table 4: Effect of HI on bead width and contact Angle of Al 6061-SS304: A Comparative Analysis of Different Process Parameters (Trails T1-T9).

Trials No.	Welding Speed (m/min)	Interval time (sec)	CMT Cycle	Heat Input (Q) J/mm	Bead Width (B) mm	Contact Angle (θ)	IMC thickness (microns)
T1	0.40	0.08	4	122	7.26	44	5.395
T2	0.40	0.10	5	122	7.35	40	7.5945
T3	0.40	0.12	6	103	6.74	46	6.7076
T4	0.45	0.10	6	113	7.15	52	7.7902
T5	0.45	0.12	4	91	6.72	74	6.7000
T6	0.45	0.08	5	131	8.41	66	9.798
T7	0.50	0.12	5	107	6.86	52	4.9113
T8	0.50	0.08	6	143	8.43	38	6.7147
T9	0.50	0.10	4	90	6.10	56	5.892

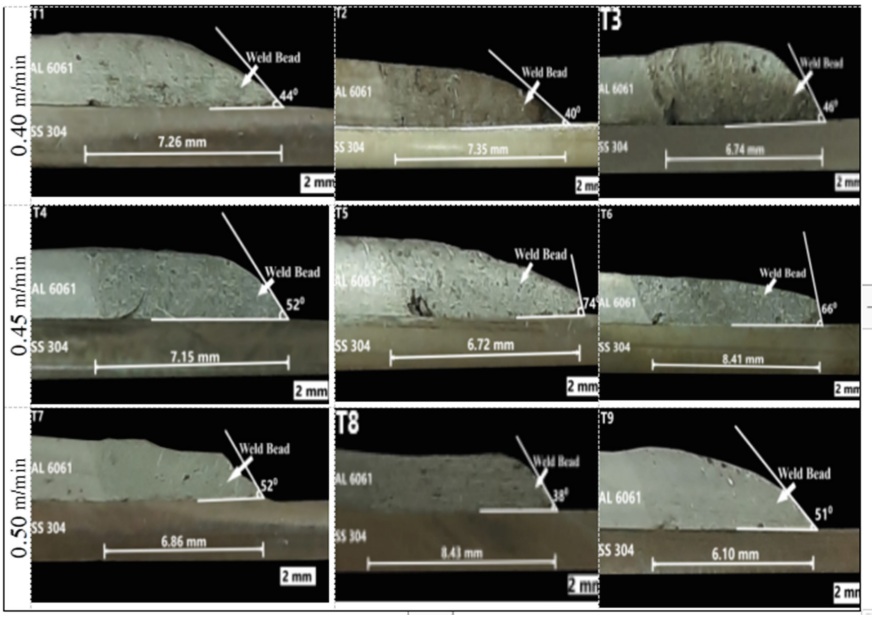

Fig. 3: Macroscopic images of a lap joint CMT welding bead of Al 6061 and SS 304.

welding bead of Al 6061 and SS 304. However, the contact angle generally decreases with increasing HI, indicating better contact of the molten metal on the substrate. This is because a higher HI promotes better mixing and bonding between the molten metal and the substrate, resulting in better contact and a lower contact angle. The weld joint was created using the pulsed CMT process with optimized process parameters. The image provided shows a cross-sectional view of a weld joint between Al 6061 and SS 304. The fusion zone profile shows a smooth and consistent surface, indicating the reliability of the joint. The influence of process parameters, including the interval time, welding speed, and CMT cycle, on the fusion zone profile is apparent. The fusion zones created using process parameters resulting in a high HI are wider and flatter than those created using process parameters resulting in a low HI. The contact angle, which is the angle between the solidified FM and the BM, also varies with the HI. As the HI increases, the contact angle decreases, indicating better contact of the FM on the BM. Figure 4 shows the relationship between heat input and weld width, as well as heat input and wetting angle for various pulse CMT process parameters of Al 6061-SS 304 joints. The curves in Fig. 4 represent how changes in heat input affect the weld width and wetting angle of the joints.

The presence of corrugated and curved shapes in the fusion zone profile is also noticeable, especially near the edges of the joint. This could be due to the non- uniform distribution of heat during welding or the interaction between the molten metal and the solidified metal. The interact between the intermetallic compound (IMC) and the fusion zone is also visible in the image. The IMC layer, which is less than 10 microns thick, is a sign of good metallurgical bonding between the BM and the FM. The IMC layer is

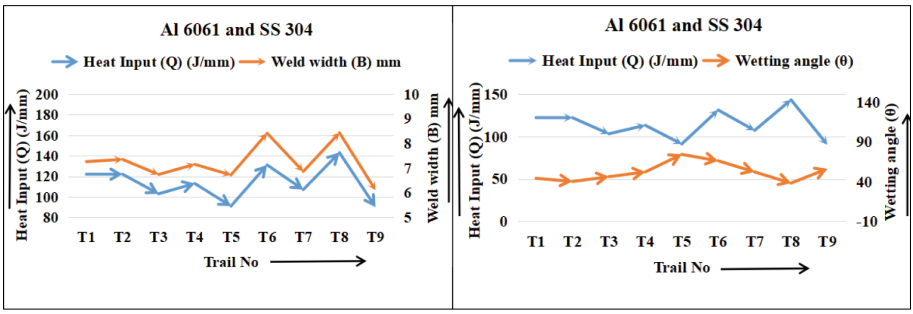

Fig. 4. HI vs Weld width and HI vs Wetting angle curves of various CMT process parameter of Al 6061-SS 304.

essential for the mechanical strength of the joint, and its thickness can be optimized by adjusting the process parameters.

3.2 Microhardness Distribution at HAZ and Fusion Zone of Al 6061-T6 and SS 304

The study investigated the microhardness and tensile strength of lap joint welding of Al 6061-T6 to electrolyte zinc coated stainless steel 304 using the pulsed CMT welding technique. The welding parameters analyzed were welding speed, interval time, and CMT cycle as shown in Table 5. The Vickers hardness testing method was used to measure the hardness values at three points: the HAZ of Al 6061-T6, the HAZ of SS 304, and the fusion zone. The results showed that the welding speed, interval time, and CMT cycle had a significant impact on the hardness values of the HAZ and fusion zone. Figure 5 compares the microhardness test results for the heat-affected zone (HAZ) of Al 6061-T6, HAZ of SS 304, and the fusion zone of the welded joints. The figure presents the microhardness values obtained from the trials conducted (T1 to T9) for each respective zone. This comparison allows for an analysis of the variations in microhardness across the different zones and provides insights into the mechanical properties of the HAZ and fusion zone of the Al 6061-T6 and SS 304 joints.

The study observed that increasing welding travel resulted in an increase in microhardness values of the HAZ and fusion zone. This was evident in the increase of HAZ of Al microhardness value from 97.4 in T1 to 116.7 in T8 with a rise in welding travel from 0.40 to 0.50 m/min. Higher welding speeds lead to reduced HI, resulting in faster cooling rates and increased microhardness values. For Trials T4 and T8 have the highest fusion zone microhardness at 132.8 and 141.6 respectively, indicating that a higher CMT cycle and welding travel have a positive effect on the fusion zone microhardness. Figure 6 shown as microhardness test samples for trials (T1 to T9) on the HAZ of Al 6061-T6, HAZ of SS 304, and the fusion zone.

The study showed that lower hardness values in the HAZ and fusion zone were observed with an increase in welding travel or a decrease in the interval time. However, an increase in the CMT cycle resulted in higher hardness values in the fusion zone, but lower values in the HAZ. Moreover, the microhardness of the HAZ of Al 6061 and

Table 5: The microhardness test results for the trials conducted (T1 to T9) on the HAZ of Al 6061-T6, HAZ of SS 316, and the weld bead.

Trials No.	Welding Speed (m/min)	Interval time (sec)	CMT Cycle	Heat Input Q) J/mm	HAZ Al 6061-T6 (HV)	HAZ SS 304 (HV)	Weld Bead (HV)
T1	0.40	0.08	4	122	97.4	139.7	119.5
T2	0.40	0.10	5	122	85.5	130.9	129.2
T3	0.40	0.12	6	103	79.1	127.7	98.5
T4	0.45	0.10	6	113	96.2	125.2	132.8
T5	0.45	0.12	4	91	116.4	123.9	104.0
T6	0.45	0.08	5	131	92.7	104.7	118.5
T7	0.50	0.12	5	107	91.7	120.3	91.7
T8	0.50	0.08	6	143	116.7	153.7	141.6
T9	0.50	0.10	4	90	100.2	132.5	110.2

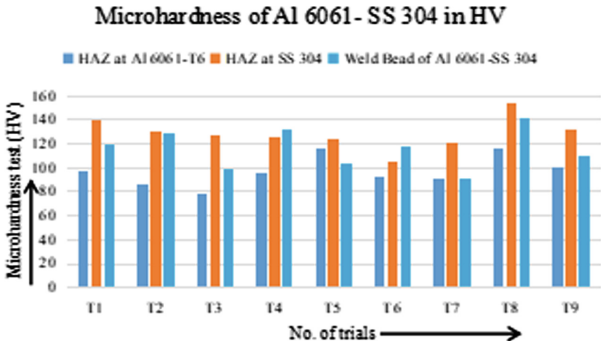

Fig. 5: A comparison of the microhardness test results for the trials conducted (T1 to T9) on the HAZ of Al 6061-T6, HAZ of SS 304, and the fusion zone.

SS 304 also varies with the input parameters. For example, Trial T8 has the highest microhardness of HAZ SS at 153.7, which could be due to the higher welding travel and CMT cycle. In trial T8, the welding travel was 0.50 m/min, interval time was 0.08 s, and CMT cycle was 6. This trial produced the highest microhardness values for both the HAZ of Al 6061 and the HAZ of SS 304, as well as the highest microhardness value for the fusion zone at 141.6.

3.3 Tensile Strength Tests on Lap Joint of Aluminum-Stainless Steel

The aim of the study was to evaluate the mechanical behavior of lap joint specimens made of aluminum 6061-T6 and stainless steel 304. To accomplish this, tensile strength tests were conducted on the specimens using a universal testing machine in accordance with

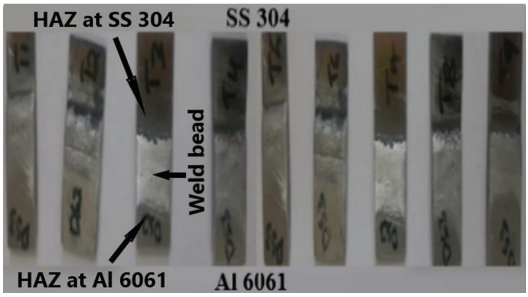

Fig. 6: Microhardness test samples for trails (T1 to T9) on the HAZ of Al 6061-T6, HAZ of SS 304, and the fusion zone.

the ASME Section 9 standard. The results of the study revealed that the fracture occurred in the brittle intermetallic compound layer of the weld fusion zone or fusion zone, which could impact the overall strength of the joint. The findings of this study are significant, as they highlight the importance of understanding the properties of the weld fusion zone in lap joint specimens made of dissimilar metals. The brittle intermetallic compound layer that formed in the fusion zone was found to be responsible for the fracture in the joint, indicating that more attention needs to be paid to the welding process and the choice of welding materials. As shown in Fig. 7, the tensile test results for trial specimens (T1 to T9) indicate failure points for Al 6061 and SS 304. Figures 8, 9, and 10 are also displays the ultimate tensile stress values, displacement values and yield stress values for the trials (T1 to T9) conducted on Al 6061 and SS 304.

The lap joints made of Al 6061-T6 and SS 304 exhibited high tensile strength values due to the strong bonding achieved through the CMT welding process. The maximum load values ranged from 2.35 kN to 4.32 kN, representing a significant variation in the strength of the lap joint. Similarly, the maximum stress values ranged from 56.884 MPa to 123.781 MPa, representing a significant variation in the stress experienced by the joint during the tensile strength test. Additionally, the yield stress values ranged from 21.08 MPa to 36.23 MPa, indicating that the lap joint in Trial 8 was able to withstand significantly more stress before experiencing plastic deformation.Table 6 shown as the results obtained from the tensile strength tests of the lap joint created by pulse CMT welding between Al 6061-T6 and SS 304. The results indicate that increasing welding travel and decreasing interval time resulted in higher maximum loads, maximum stresses, and yield stresses. For example, in trial T8, where the welding travel was 0.50 m/min and the interval time was 0.08 s, the lap joint had a maximum load of 4.32 KN, a maximum stress of 123.781 MPa, and a yield stress of 36.23 MPa.

4 Conclusions

The study used the pulsed CMT process to weld dissimilar materials, aluminium alloy Al 6061-T6 and electrolytic Zn-coated stainless steel SS 304 was effective in defect free welding. The welding parameters, including welding speed, interval time, and CMT cycle, were varied to investigate their effect on the mechanical and microstructural properties of the joint.

Table 6: The results obtained from the tensile strength tests of the lap joint created by pulse CMT welding between Al 6061-T6 and SS 304.

Trials No.	Welding Speed (m/min)	Interval time in sec	CMT Cycle	Heat Input(Q) J/mm	Maximum Load in KN	Ultimate tensile Stress in MPa	Yield Stress in MPa	Displacement in mm
T1	0.40	0.08	4	122	2.82	88.24	30.12	1.4
T2	0.40	0.10	5	122	3.06	90.057	28.89	0.3
T3	0.40	0.12	6	103	3.13	92.119	26.63	2.7
T4	0.45	0.10	6	113	2.35	56.884	21.08	0.7
T5	0.45	0.12	4	91	2.93	84.947	25.12	1.6
T6	0.45	0.08	5	131	3.15	92.12	29.87	2.0
T7	0.50	0.12	5	107	3.16	100.014	31.12	1.4
T8	0.50	0.08	6	143	4.32	123.781	36.23	2.6
T9	0.50	0.10	4	90	2.97	78.428	25.81	1.7

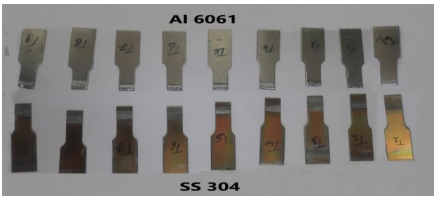

Fig. 7: Tensile test results for trial specimens (T1 to T9) at failure of (Al 6061 and SS 304)

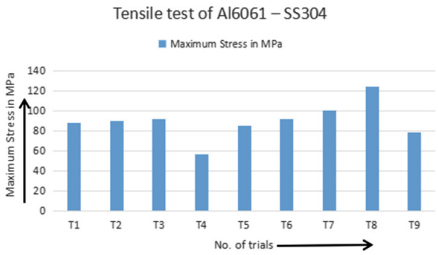

Fig. 8: Ultimate tensile stress of Al 6061 and SS 304 for the trials (T1 to T9)

1) The results show that the bead width and contact angle are dependent on the HI and the combination of welding parameters used. For example, joint T8 produced with a welding travel of 0.50 m/min, interval duration of 0.08 s, and CMT cycle stage of 6 had the largest bead width of 8.43 mm and the smallest contact angle of 38 degrees. On the other hand, joint T5 produced with a welding travel of 0.45 m/min, interval

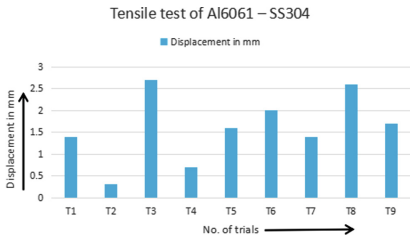

Fig. 9: Displacement of Al 6061 and SS 304 for the trials (T1 to T9)

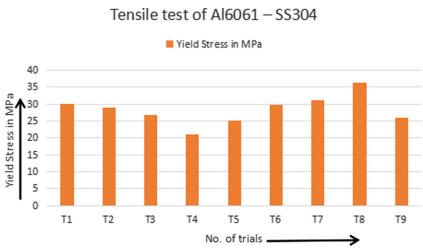

Fig. 10: Yield stress of Al 6061 and SS 304 for the trials (T1 to T9)

duration of 0.12 s, and CMT cycle stage of 4 had the smallest bead width of 6.72 mm and the largest contact angle of 74 degrees.

2) The results suggest that increasing the HI generally leads to an increase in the bead width, which is expected since more HI results in more melting and flow of molten metal. However, the contact angle generally decreases with increasing HI, indicating better contact of the molten metal on the substrate. This is because a higher HI promotes better mixing and bonding between the molten metal and the substrate, resulting in better contact and a lower contact angle.
3) The results showed that increasing welding travel resulted in higher microhardness values of the HAZ and fusion zone, and higher CMT cycle and welding travel had a positive effect on the fusion zone microhardness.
4) The microhardness of the HAZ of Al 6061 and SS 304 also varies with the input parameters. For example, Trial T8 has the highest microhardness of HAZ SS at 153.7, which could be due to the higher welding travel and CMT cycle. In trial T8, the welding travel was 0.50 m/min, interval time was 0.08 s, and CMT cycle was 6. This trial produced the highest microhardness values for both the HAZ of Al 6061 and the HAZ of SS 304, as well as the highest microhardness value for the fusion zone at 141.6.
5) The microhardness of the HAZ of both materials also varied with the input parameters. Increasing welding travel and decreasing interval time resulted in higher maximum loads, maximum stresses, and yield stresses.
6) The results indicate that increasing welding travel and decreasing interval time resulted in higher maximum loads, maximum stresses, and yield stresses. For example, in trial T8, where the welding travel was 0.50 m/min and the interval time

was 0.08 s, the lap joint had a maximum load of 4.32 KN, a maximum stress of 123.781 MPa, and a yield stress of 36.23 MPa.

7) The tensile strength of the joint was found to be influenced by the microstructure and microhardness values of the welded joint. The highest microhardness values and tensile strength were obtained in Trial T8, where the welding travel was 0.50 m/min, interval time was 0.08 s, and CMT cycle was 6.
8) The resulting welds had different intermetallic compound (IMC) and bead interact morphologies. The fusion zones had corrugated and curved shapes and were more prominent at the joints, while the IMC at the Al 6061-T6 and SS 304 interact were less than 10 microns.

References

1. Miller WS, Zhuang L, Bottema J, Wittebrood A, De Smet P, Haszler A, Vieregge AJ. Recent development in aluminium alloys for the automotive industry. Materials Science and Engineering: A. 280(1): 37–49. Author, F.: Article title. Journal 2(5), 99–110 (2016).
2. Schubert E, Klassen M, Zerner I, Walz C, Sepold G. Light-weight structures produced by laser beam joining for future applications in automobile and aerospace industry. Journal of Materials Processing Technology: 115(1), 2–8 (2001).
3. Maisonnette, D., Suery, M., Nelias, D., Chaudet, P., & Epicier, T. "Effects of Heat Treatments on the Microstructure and Mechanical Properties of a 6061 Al Alloy", Materials Science and Engineering: A, 528(6), 2718–2724, 2011.
4. Das A, Shome M, Goecke SF, De A. Joining of aluminium alloy and galvanized steel using a controlled gas metal arc process. Journal of Manufacturing Processes: 27, 179–87 (2017).
5. Song JL, Lin SB, Yang CL, Fan CL. Effects of Si additions on intermetallic compound layer of aluminum–steel TIG welding–brazing joint. Journal of Alloys and Compounds: 488(1), 217–22 (2009).
6. Zhang Y, Huang J, Cheng Z, Ye Z, Chi H, Peng L, Chen S. Study on MIG-TIG double-sided arc welding-brazing of aluminum and stainless steel. Materials Letters: 172, 146–8 (2016).
7. Zhang HT, Feng JC, He P. Interfacial phenomena of cold metal transfer (CMT) welding of zinc coated steel and wrought aluminium. Materials science and technology: 24(11), 1346–9 (2008).
8. Zhao D, Ren D, Zhao K, Pan S, Guo X. Effect of welding parameters on tensile strength of ultrasonic spot welded joints of aluminum to steel–By experimentation and artificial neural network. Journal of Manufacturing processes: 30, 63–74 (2017).
9. Xia H, Tao W, Li L, Tan C, Zhang K, Ma N. Effect of laser beam models on laser welding–brazing Al to steel. Optics & Laser Technology: 122, 105845 (2020).
10. Hussein SA, Hadzley AB. Characteristics of aluminum-to-steel joint made by friction stir welding: A review. Materials Today Communications: 5, 32–49 (2015).
11. Hussein SA, Hadzley AB. Characteristics of aluminum-to-steel joint made by friction stir welding: A review. Materials Today Communications: 5, 32–49 (2009).
12. Basak S, Das H, Pal TK, Shome M. Characterization of intermetallics in aluminum to zinc coated interstitial free steel joining by pulsed MIG brazing for automotive application. Materials Characterization: 112, 229–237 (2016).
13. Mathieu A, Shabadi R, Deschamps A, Suery M, Matteï S, Grevey D, Cicala E. Dissimilar material joining using laser (aluminum to steel using zinc-based filler wire). Optics & Laser Technology: 39(3), 652–661 (2007).

14. Li J, Shen J, Hu S, Liang Y, Wang Q. Microstructure and mechanical properties of 6061/7N01 CMT+ P joints. Journal of Materials Processing Technology: 264, 134–144 (2019).
15. Cao R, Huang Q, Zeng CZ, Ai BQ, Lin Q, Chen JH, Wang PC. Cold metal transfer plug welding of aluminum AA6061-T6-to-bare mild steel. Journal of Manufacturing Science and Engineering: 138(8), 2016.
16. Yagati KP, Bathe R, Joardar J, Phaniprabhakar KV, Padmanabham G. Al–Steel Joining by CMT Weld Brazing: Effect of Filler Wire Composition and Pulsing on the Interact and Mechanical Properties. Transactions of the Indian Institute of Metals: 72(10), 2763–2772 (2019).
17. Yang J, Yu Z, Li Y, Zhang H, Guo W, Zhou N. Influence of alloy elements on microstructure and mechanical properties of Al/steel dissimilar joint by laser welding/brazing. Welding in the World: 62(2), 427–433 (2018).
18. Yagati KP, Bathe RN, Rajulapati KV, Rao KB, Padmanabham G. Fluxless arc weld-brazing of aluminium alloy to steel. Journal of Materials Processing Technology: 214(12), 2949–2959 (2014).
19. Cao R, Huang Q, Chen JH, Wang PC. Cold metal transfer spot plug welding of AA6061-T6-to-galvanized steel for automotive applications. Journal of Alloys and Compounds: 585, 622–632 (2014).